Failure probability estimation of dynamic systems employing relaxed power spectral density functions with dependent frequency modeling and sampling

Marco Behrendt[a], Meng-Ze Lyu[b,c,*], Yi Luo[a], Jian-Bing Chen[b,c], Michael Beer[a,d,e]

[a] *Institute for Risk and Reliability, Leibniz Universität Hannover, Callinstraße 34, 30167 Hannover, Germany*
[b] *State Key Laboratory of Disaster Reduction in Civil Engineering, Tongji University, 1239 Siping Road, Shanghai 200092, China*
[c] *College of Civil Engineering, Tongji University, 1239 Siping Road, Shanghai 200092, China*
[d] *Institute for Risk and Uncertainty, University of Liverpool, Peach Street, Liverpool L69 7ZF, United Kingdom*
[e] *International Joint Research Center for Resilient Infrastructure & International Joint Research Center for Engineering Reliability and Stochastic Mechanics, Tongji University, 1239 Siping Road, Shanghai 200092, China*

Abstract

This work addresses the critical task of accurately estimating failure probabilities in dynamic systems by utilizing a probabilistic load model based on a set of data with similar characteristics, namely the relaxed power spectral density (PSD) function. A major drawback of the relaxed PSD function is the lack of dependency between frequencies, which leads to unrealistic PSD functions being sampled, resulting in an unfavourable effect on the failure probability estimation. In this work, this limitation is addressed by various methods of modeling the dependency, including the incorporation of statistical quantities such as the correlation present in the data set. Specifically, a novel technique is proposed, incorporating probabilistic dependencies between different frequencies for sampling representative PSD functions, thereby enhancing the realism of load representation. By accounting for the dependencies between frequencies, the relaxed PSD function enhances the precision of failure probability estimates, opening the opportunity for a more robust and accurate reliability assessment under uncertainty. The effectiveness and accuracy of the proposed approach is demonstrated through numerical examples, showcasing its ability to provide reliable failure probability estimates in dynamic systems.

Keywords: Power spectral density function, Stochastic processes, Stochastic dynamics, Uncertainty quantification, Probabilistic dependency.

1. Introduction

Stochastic dynamics investigates the behavior of systems under the influence of random vibrations and introduces a crucial element of unpredictability into the study of dynamic phenomena, which is often concerned with reliability analysis of a given structure [1, 2, 3, 4]. Unlike deterministic systems, where the future behavior is completely determined by the initial conditions, stochastic dynamics incorporates the element of randomness, making it a powerful tool for modeling real-world phenomena characterized by inherent uncertainties. Random vibrations [5, 6, 7, 8, 9] constitute a significant aspect of stochastic dynamics in structural engineering and dynamic analysis. These vibrations are often induced by external factors such as wind, seismic activity, or other environmental forces, introducing a level of unpredictability that demands a stochastic approach for accurate modeling and analysis. Environmental processes represent notable examples in which stochastic dynamics plays a crucial role, particularly when considering their impact on buildings and structures. These natural phenomena are inherently complex, characterized by intricate patterns of variability and randomness that challenge traditional deterministic models.

In structural reliability and stochastic dynamics, the power spectral density (PSD) function is an important tool in characterizing and understanding the dynamics of the underlying process and the response of structure and can be derived directly from environmental processes [9, 10]. This statistical measure provides a representation of environmental excitations in the frequency domain and allows the reliability of structures to be assessed under random loading conditions. By analyzing the PSD function, insight can be gained into the distribution of energy across different frequencies, allowing the identification of critical resonances and potential weaknesses in structural systems. This information is invaluable for the design

*Corresponding author
Email address: lyumz@tongji.edu.cn (Meng-Ze Lyu)

and assessment of structures and improves the ability to simulate and mitigate the effects of random excitations on the built environment. In this type of analysis, it is beneficial to use methods that generate compatible stochastic processes from an underlying PSD function for the application to structures. These methods are valuable as they encompass the properties of the PSD function in the time domain, see for instance the spectral representation method [11] or the stochastic harmonic functions [12, 13].

The challenges posed by uncertainties in stochastic dynamics and PSD function estimation are manifold and are paramount in understanding and predicting the behavior of complex systems. These uncertainties, which are usually divided into aleatory and epistemic uncertainties [14], can arise from various sources, such as measurement errors, environmental fluctuations, or incomplete knowledge of the underlying system [15]. As a result, accurately modeling and analyzing stochastic processes becomes a non-trivial task. The key challenges are the correct treatment of uncertainties [16, 17] and the formulation of mathematical models that capture the stochastic nature of loads subject to the system while accounting for uncertainties, see [18, 19, 20, 21] for an overview. Traditional deterministic models often prove insufficient in representing the inherent variability observed in many natural and engineered systems. Various approaches for handling uncertainties are outlined in the literature, and they can be broadly categorized into distinct groups, including probabilistic approaches [19], which quantify uncertainties using probability distributions; non-probabilistic approaches [22], which do not rely on explicit probability measures; and imprecise probabilistic approaches [23], which account for uncertainties using set-valued or imprecise probability representations. Some specific methods to determine the structural reliability under uncertainties are the Monte Carlo (MC) method [24, 25], subset simulation (SuS) [26, 27], line sampling [28], or Bayesian methods [29, 30].

Accurately quantifying and incorporating uncertainties into the PSD function, which serves as a load model under specific conditions, presents a challenging task. Incorrect quantification and insufficient consideration of uncertainties can lead to significant consequences in determining the structural reliability. Missing data, for instance, is problem in statistical analyses as it affects the accuracy and reliability of the results due to gaps in the data set, which can lead to biased conclusions and low statistical significance. This problem is tackled by different approaches such as artificial neural networks [31], probabilistic modeling [32, 33] and compressive sensing [34, 35]. In some cases, there may be a lack of available information, or the data at hand might not be sufficiently precise. In such cases, it is beneficial to consider the parameters of a PSD function as intervals, resulting in an imprecise load that can be used to determine bounds for the failure probability [36]. An approach for bounding limited data of estimated PSD functions was recently presented by some of the authors of this work [37]. An interval-values PSD function was proposed in [38], which is determined by a large set of accelerograms, leading to an imprecise PSD function.

Another approach proposed by some of the authors of this work is the so-called relaxed PSD function [39]. It serves as a tool for probabilistic uncertainty quantification of an ensemble of similar PSD functions. However, a significant drawback of this method is the lack of consideration for correlations between frequencies or the modeling of dependencies. In this work, this limitation is addressed by incorporating different methods for dependency modeling. In particular, a novel approach is presented that takes into account correlations between neighboring frequencies which results in accurately modeling the dependencies within the ensemble of PSD functions. Further, this strategy can be utilized to sample realistic PSD functions from the relaxed PSD function. This enhancement is crucial for a more comprehensive and realistic assessment of uncertainties in the underlying data and the determination of structural reliability.

This work is organized as follows: Section 2 introduces some basic concepts required for this work. In Section 3 different dependency modeling and sampling techniques for the relaxed PSD function are presented. Based on this methodology, numerical examples are carried out in Section 4. Some final remarks are given in Section 5.

2. Preliminaries

Some basic concepts and theoretical background required for this work is provided in this section. This includes the estimation of PSD functions, the derivation of the relaxed PSD function, the generation of stochastic processes and the failure probability estimation.

2.1. Power spectral density estimation

The Wiener-Khintchine theorem states that for a wide-sense stationary random process, the PSD function $S_X(\omega)$ of that process is the Fourier transform of its autocorrelation function $R_X(\tau)$. Mathematically, it can be expressed as follows

$$\begin{aligned} S_X(\omega) &= \int_{-\infty}^{\infty} R_X(\tau) e^{-i\omega\tau} \mathrm{d}\tau, \\ R_X(\tau) &= \frac{1}{2\pi} \int_{-\infty}^{\infty} S_X(\omega) e^{i\omega\tau} \mathrm{d}\omega, \end{aligned} \tag{1}$$

where ω is the frequency, τ is the time lag and $i = \sqrt{-1}$ is the complex number. While the Wiener-Khintchine theorem provides a theoretical framework for calculating the PSD function from the autocorrelation function, practical applications often require estimating the PSD function from finite data samples. Many of these estimators rely on the discrete Fourier transform, such as the periodogram [3, 9]

$$\hat{S}_X(\omega_k) = \lim_{T\to\infty} \frac{\Delta t^2}{T} \left| \sum_{n=0}^{N-1} x_n e^{-2\pi i k n/N} \right|^2, \tag{2}$$

where $\omega_k = \frac{2\pi k}{T}$ is the discrete frequency with integer frequency k, T is the total length of the record x_n, Δt is the time discretization, N is the total number of data points and n is the index in the record. Other methods constitute estimates in an averaged sense only, see for instance Bartlett's method [40, 41] or Welch's method [42], which is utilized in this work due to it's flexibility in segmenting the underlying signal.

In Welch's method, the signal x_n undergoes division into K segments, denoted as $x_n^{(1)} = x(n^*)$, $x_n^{(2)} = x(n^* + D)$, …, $x_n^{(K)} = x(n^* + (K-1)D)$, where $n^* = 0, 1, \ldots, L-1$. Here, L signifies the length of each individual segment, and D is a parameter determining the spacing between the starting points of the segments. Notably, D governs the extent of overlap between consecutive segments; for instance, $D = L/2$ corresponds to a 50% overlap. Each segment is multiplied by a window function $W(n^*)$. For tailoring the PSD function estimation to specific requirements, the selection of the window function is crucial. Two suggested window functions in [42] are

$$W_1(j) = 1 - \left(\frac{j - \frac{L-1}{2}}{\frac{L+1}{2}} \right)^2 \tag{3}$$

and

$$W_2(j) = 1 - \left| \frac{j - \frac{L-1}{2}}{\frac{L+1}{2}} \right|, \tag{4}$$

where $|\cdot|$ denotes the absolute value and $j = 0, 1, \ldots, L-1$. Both window functions prioritize weighting values in the center of the segment more heavily than the outer values, resulting in a further smoothing effect during the estimation process. Utilizing these window functions the calculations take the form

$$\hat{S}_X^W(\omega_m) = \frac{1}{K} \sum_{k=1}^{K} \frac{1}{L} \left| \sum_{n^*=0}^{L-1} x_k(n^*) W(n^*) e^{\frac{-2\pi i m n^*}{L}} \right|^2, \tag{5}$$

with $\omega_m = \frac{2\pi m}{T}$, equivalently to ω_k in Eq. 2.

2.2. Relaxed PSD function

The relaxed PSD function, developed by some of the authors of this work, is a probabilistic PSD function load model which aims to quantify uncertainties within data in the frequency domain [39]. The model utilizes an ensemble of N_{E} estimated PSD functions $S^{(i)}$, with $i = 1, 2, \ldots, N_{\mathrm{E}}$, which exhibit similarities in frequency domain, such as peak frequency or general shape. Based on this data, a probabilistic representation of this data set is derived, i.e. the data set is represented by a probability density function for each discrete frequency to capture the variation in the spectral density value.

For the generation of the relaxed PSD function it is required to compute the mean μ_{ω_n} and standard deviation σ_{ω_n} for each discrete frequency ω_n, such that

$$\mu_{\omega_n} = \frac{1}{N_{\mathrm{E}}} \sum_{i=1}^{N_{\mathrm{E}}} S^{(i)}(\omega_n) \tag{6}$$

and

$$\sigma_{\omega_n} = \sqrt{\frac{1}{N_{\mathrm{E}}} \sum_{i=1}^{N_{\mathrm{E}}} \left(S^{(i)}(\omega_n) - \mu_{\omega_n}\right)^2}, \tag{7}$$

with $\omega_n = n\Delta\omega$ and $n = 1, 2, \ldots, N_\omega$, where N_ω the number of discrete frequency points. By analyzing the statistical information obtained from the ensemble, it becomes possible to generate a probability distribution function for each frequency. In this work, a truncated normal distribution is employed, with truncation bounds $a = 0$ and $b = \infty$ to ensure, that negative values are excluded due to the non-negative nature of PSD functions. For a detailed description of the relaxed PSD function refer to [39].

2.3. Stochastic process generation

In stochastic dynamics the generation of stochastic processes from a specified PSD function is fundamental for understanding and simulating the inherent randomness in dynamic systems and offering insights into their behavior and performance. The spectral representation method (SRM) is a valuable technique, particularly in the context of stochastic processes [11]. This method allows for the generation of stochastic processes based on a PSD function $S(\omega)$. The process is mathematically represented by

$$x(t) = \sqrt{2} \sum_{n=0}^{N-1} (2S(\omega_n)\Delta\omega)^{1/2} \cos(\omega_n t + \phi_n), \tag{8}$$

where ω_n is the discrete frequency, $\Delta\omega = \omega_{\mathrm{u}}/N$ represents frequency discretization, ω_{u} is the upper cut-off frequency, $n = 0, 1, \ldots, N-1$ denotes the frequency steps, N is the total number of frequency points, t is the time vector and $\phi_n \sim \mathcal{U}(0, 2\pi)$ denote uniformly distributed random variables in the interval $[0, 2\pi]$.

2.4. Failure probability estimation

Stochastic dynamics plays a crucial role in modeling complex systems that are subject to uncertain and random influences. The structural behavior of many systems is determined by the inherent random phenomena. Estimating the failure probability of such systems is of paramount importance to ensure their reliability and optimal design. The failure probability indicates the likelihood that a system will exceed certain critical thresholds, which leads to an undesirable outcome, for instance that the structural reliability can not be guaranteed anymore. Accurate estimation of this probability is essential for risk assessment.

However, conventional deterministic methods are often unable to capture the full range of uncertainties present in real systems. To address these challenges, sophisticated techniques have been developed in the field of stochastic dynamics. By taking into account the inherent randomness and uncertainties, these methods provide a quantitative assessment of the failure probability and a deeper insight into the reliability of the system.

To describe the failure of a system and the corresponding failure probability (see for instance [3]), a classical failure criterion is the first-passage probability. This describes the probability that the system under investigation exceeds a pre-defined threshold in the quantity of interest, e.g. the displacement of a specific storey of a building or its inter-storey drift. This problem can be described by

$$F_{\mathrm{s}} = \Pr\{y(t) \in \Omega_{\mathrm{s}}, t \in (0, T]\}, \tag{9}$$

where $y(t)$ is assumed to be the response of a system, Ω_{s} is the safe domain, i.e. the range of responses where the system is safe, t is the time variable and T as the total duration of the investigated time frame. If the response exceeds the safe domain, the system is assumed to fail.

The estimation of the failure probability is an essential part in stochastic dynamics. It leads to results to conclude about the safety of a building or structure and determines the safety margins. In the case of first-passage problems the system responses $y(t)$ of a stochastic input $x(t)$ are investigated whether they exceed the pre-defined threshold. Therefore, the so-called performance function $g(x)$ is determined, which is often referred to as limit state function. If $g(x) < 0$, the system is assumed to fail, while $g(x) \geq 0$ determines a safe event. If precise probabilistic is considered, the failure probability p_{f} can be determined by

$$p_{\mathrm{f}} = \int_{\mathcal{X}} I(x) f(x) \mathrm{d}x. \tag{10}$$

The failure probability is mainly governed by the probability density function (PDF) $f(x)$ of the random variables and the indicator function $I(x)$, which is assigned the value 1 if the system is assumed to fail and 0 if not, namely,

$$I(x) = \begin{cases} 1, & g(x) \leq 0, \\ 0, & \text{otherwise.} \end{cases} \tag{11}$$

The MC method stands out as one of the most widely recognized stochastic simulation techniques, see [24] for an overview. MC is known to be a robust sampling procedure for the failure probability by applying the following expression as

$$p_{\mathrm{f}}^{\mathrm{MC}} = \frac{1}{n} \sum_{i=1}^{n} I\left(x^{(i)}\right). \tag{12}$$

However, in particular for the efficient determination of small failure probabilities MC has its limitations. In this case, MC is impractical because an prohibitively high number of samples $N_{\mathrm{MC}} \approx \frac{1}{p_{\mathrm{f}}}$ may be required to determine the failure probability. For this purpose, advanced sampling techniques such as SuS [26] were developed to overcome this issue.

3. Dependency modeling and sampling in relaxed PSD functions

In its current form, the relaxed PSD function does not take dependencies or correlations into account, which is a major drawback for accurately modeling of loads subject to systems where interrelationships among variables play a crucial role in understanding the overall behavior. Addressing this limitation would enhance the model's ability to capture nuanced interactions and improve its applicability to more realistic scenarios. Thus, various approaches to account for dependencies are considered here, with the proposed method being universally applicable to diverse forms of PSD functions, including seismic spectra, wind spectra, and wave spectra. In the following, a randomly generated set of earthquake data is utilized for illustration purposes.

Sampling without accounting for correlations or modeled dependencies leads to a high variability in samples, as illustrated in Fig. 1. It becomes imperative to consider correlations and model dependencies accurately, as this significantly impacts the reliability and precision of the sampled data. The incorporation of correlations ensures a more realistic representation of the underlying characteristics. This consideration becomes particularly crucial in scenarios where the interactions and dependencies between frequencies contribute significantly to the load's behavior.

3.1. One random variable

A simple form of a sampling procedure under dependency modeling is the utilization of only one random variable in the sampling process. In this case X is a random variable with a

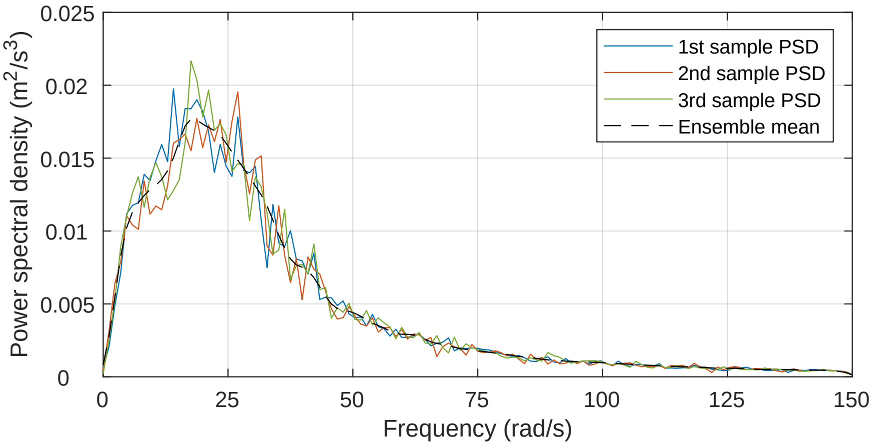

Figure 1: Generated samples without dependency modeling or consideration of correlations.

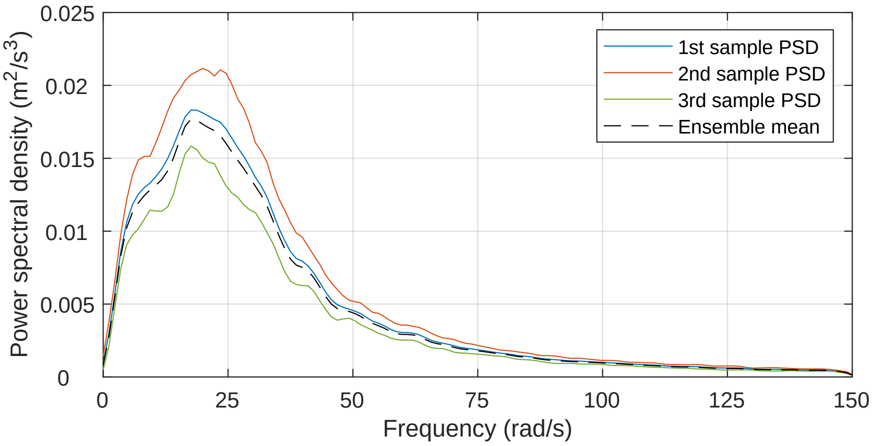

Figure 2: Generated sample PSD functions for the one RV model.

cumulative distribution function (CDF) $F(x)$ corresponding to the PDF. The inverse CDF, $F^{-1}(u)$, can be computed, where $u \sim \mathcal{U}(0, 1)$ is a uniformly distributed random variable on the interval $[0, 1]$. A random sample of u is generated and $X = F^{-1}(u)$ is computed. This process ensures that X will have the desired distribution according to the given PDF. If a random number is generated and sampled from each inverse CDF of the individual spectral densities in the relaxed PSD function, "slices" of the PSD function are sampled, which have the same probability density when all PDFs are normalized. Although this procedure does not consider the correlations between frequencies, it is a simple method to effectively model dependencies. The generated samples are depicted in Fig. 2.

An advantage of this method is obviously the utilization of only $N_{\mathrm{Z}} = 1$ random variable for each PSD function sample. In addition, very smooth realizations can be obtained. However, the smoothness of the samples depends highly on the shape of the relaxed PSD function itself, as other data sets can result in relaxed PSD functions which exhibit a higher variation. In addition, correlations within the data set, if existing, are not considered and the approach may lack flexibility and coverage of the full probability space. For the remainder of this work, the model is referred to as *one random variable (RV) model*.

3.2. Multivariate Gaussian distribution

Another approach is the modeling of a multivariate Gaussian distribution based on the marginal PDFs of the relaxed PSD function under consideration of correlations. The multivariate Gaussian distribution for a vector of random variables $\boldsymbol{X} = [X_1, X_2, ..., X_p]$ with mean vector $\boldsymbol{\mu_X} = [\mu_1, \mu_2, ..., \mu_p]$ and covariance matrix $\boldsymbol{\Sigma_X}$ is given by

$$f(\boldsymbol{x}) = \frac{1}{\sqrt{(2\pi)^p \det(\boldsymbol{\Sigma_X})}} \exp\left(-\frac{1}{2}(\boldsymbol{x} - \boldsymbol{\mu_X})^T \boldsymbol{\Sigma_X}^{-1} (\boldsymbol{x} - \boldsymbol{\mu_X})\right), \tag{13}$$

with $\boldsymbol{x}$ as vector of random variables and p as the dimensionality of the distribution. This equation describes the joint PDF of observing the vector of random variables $\boldsymbol{x}$ in a multivariate Gaussian distribution. The mean vector $\boldsymbol{\mu_X}$ represents the center of the distribution, and the covariance matrix $\boldsymbol{\Sigma_X}$ captures the relationships and variances between the different variables.

To sample from this multivariate Gaussian distribution the Cholesky decomposition can be used to transform independent standard Gaussian random variables into correlated Gaussian variables. This technique involves decomposing the covariance matrix $\boldsymbol{\Sigma_X}$ into the product of a lower triangular matrix $\boldsymbol{L}$ and its transpose $\boldsymbol{L}^T$, such that $\boldsymbol{\Sigma_X} = \boldsymbol{L}\boldsymbol{L}^T$. The sampled multivariate Gaussian random variables $\boldsymbol{x}$ can be obtained by generating a vector of p independent standard Gaussian random variables, denoted as $\boldsymbol{z} = [z_1, z_2, ..., z_p]$. Next, the standard Gaussian random variables are transformed using the Cholesky decomposition: $\boldsymbol{x} = \boldsymbol{\mu} + \boldsymbol{L}\boldsymbol{z}$. This transformation ensures that $\boldsymbol{x}$ follows a multivariate Gaussian distribution with mean vector $\boldsymbol{\mu_X}$ and covariance matrix $\boldsymbol{\Sigma_X}$.

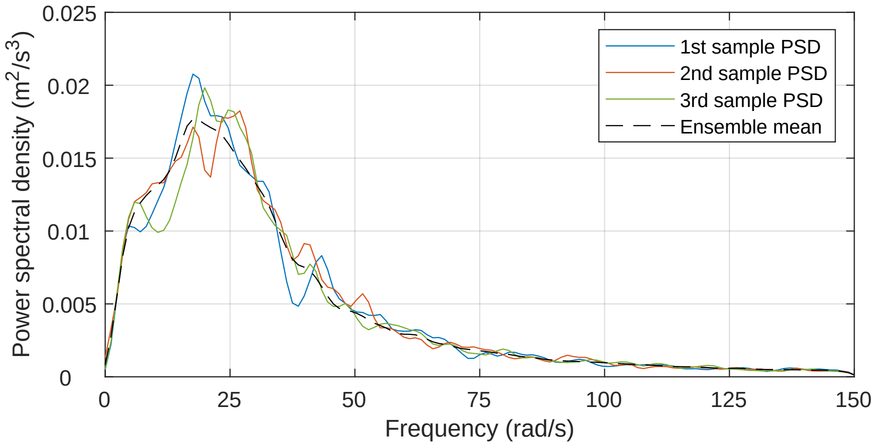

Figure 3: Generated sample PSD functions for the MVG model.

The Cholesky decomposition not only simplifies the sampling process but also guarantees positive definiteness, ensuring the validity of the resulting covariance matrix. The correlation is comprehensively addressed through the Cholesky decomposition of the covariance matrix. This approach provides an efficient and numerically stable method for generating samples. A number of $N_\mathrm{Z} = p$ random variables is required. An example of samples using this approach is given in Fig. 3. However, it should be noted that for the use of multivariate Gaussian distributions, the data must exhibit a certain correlation, which may not be guaranteed when using PSD function estimators that lead to poor quality results. In the following, the model is referred to as *multivariate (MVG) model.*

3.3. Proposed sampling procedure

In the following, a novel approach for sampling PSD functions considering correlations is presented, which is tailored specifically for the use in the relaxed PSD function. Through the uncertainty modeling of the relaxed PSD function using observed data, the mean $\mu_S(\omega)$, the variance $\sigma_S^2(\omega)$ and the covariance $\varsigma_S(\omega, \omega + \Delta\omega)$ can be obtained

$$\begin{cases} \mu_S(\omega) = \mathrm{E}[S(\omega)], \\ \sigma_S^2(\omega) = \mathrm{E}[S^2(\omega)] - \mathrm{E}^2[S(\omega)], \\ \varsigma_S(\omega, \omega + \Delta\omega) = \mathrm{E}[S(\omega)S(\omega + \Delta\omega)] - \mathrm{E}[S(\omega)]\,\mathrm{E}[S(\omega + \Delta\omega)], \end{cases} \tag{14}$$

where E[$\cdot$] is the expectation operator. Those statistical quantities are deterministic functions with respect to ω given by the relaxed PSD function via observed data determined at discrete points ω_i, for $i = 1, 2, \ldots, N_\omega$. Here and in the following $S(\omega_i) \widehat{=} S_i$, $\mu_S(\omega_i) \widehat{=} \mu_i$, $\sigma_S(\omega_i) \widehat{=} \sigma_i$ and $\varsigma_S(\omega_i, \omega_{i+1}) \widehat{=} \varsigma_{i,i+1}$ for simplicity.

The approach is able to model dependencies between neighboring frequencies only. By doing so, the sampling procedure is improved. The proposed PSD function sampling method belongs to the category of Markov sampling, where the obtained PSD function can be seen as a sample path of a non-stationary Ornstein-Uhlenbeck process with respect to frequency.

The first PSD function value $S_1 \sim \mathcal{N}(\mu_1, \sigma_1^2)$ is sampled in accordance with the respective determined PDF of the relaxed PSD function. The next PSD function value S_2 can be obtained by adding S_1 and a specified term ΔS_1 which accounts for the correlation between S_1 and S_2. This procedure can be continued for S_3, S_4, ..., S_{N_ω}, until the entire PSD function is sampled.

In general, the sampling procedure reads

$$S_{j+1} = S_j + \Delta S_j, \tag{15}$$

where the term ΔS_j is described by

$$\Delta S_j = -k_j S_j + \lambda_j \varPhi_j + \mu_{j+1} - (1 - k_j)\mu_j, \tag{16}$$

with $\varPhi_j \sim \mathcal{N}(0, 1)$ for $j = 1, \ldots, N_\omega - 1$. For Eq. 15 and 16, the determination of the newly introduced parameters k_j and λ_j is required. Therefore, the following conditions for the variance

$$\begin{aligned} \mathrm{Var}(S_{j+1}) = \sigma_{j+1}^2 &= (1 - k_j)^2 \underbrace{\mathrm{Var}(S_j)}_{=\sigma_j^2} + \lambda_j^2 \underbrace{\mathrm{Var}(\varPhi)}_{=1} \\ &= (1 - k_j)^2 \sigma_j^2 + \lambda_j^2 \end{aligned} \tag{17}$$

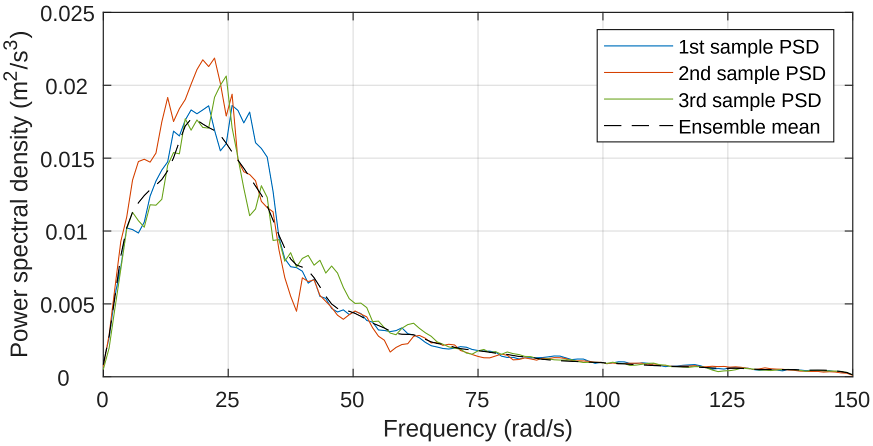

Figure 4: Generated sample PSD functions for the proposed sampling approach.

and for the cross-correlation between neighboring frequencies

$$\begin{aligned}
\mathrm{E}[S_j S_{j+1}] &= \mathrm{Cov}(S_j, S_{j+1}) + \mathrm{E}[S_j]\,\mathrm{E}[S_{j+1}] \\
&= \varsigma_{j,j+1} + \mu_j \mu_{j+1} \\
&= (1-k_j)\underbrace{\mathrm{E}[S_j^2]}_{=\mu_j^2+\sigma_j^2} + \lambda_j \underbrace{\mathrm{E}[S_j \Phi]}_{=0} + (\mu_{j+1} - (1-k_j)\mu_j)\underbrace{\mathrm{E}[S_j]}_{=\mu_j} \\
&= (1-k_j)(\mu_j^2 + \sigma_j^2) + \mu_j \mu_{j+1} - (1-k_j)\mu_j^2 \\
&= \mu_j \mu_{j+1} + (1-k_j)\sigma_j^2
\end{aligned} \tag{18}$$

are introduced. Reformulation of Eqs. 17 and 18 will yield a system of linear equations with two unknowns, which are the paramter λ_j and k_j

$$\begin{cases} k_j = 1 - \dfrac{\varsigma_{j,j+1}}{\sigma_j^2}, \\ \lambda_j = \sqrt{\sigma_{j+1}^2 - \dfrac{\varsigma_{j,j+1}}{\sigma_j^2}}, \end{cases} \quad \text{for } j = 1, \ldots, N_\omega - 1. \tag{19}$$

The system of linear equations can be solved to obtain the values of λ_j and k_j and the subsequent PSD function value S_{j+1} can be evaluated by Eq. 15. This procedure has to be repeated until S_{N_ω} has been reached and a PSD function is being sampled. An example of sampled PSD functions is given in Fig. 4.

The sampled PSD functions are sufficiently smooth and they do not show irregular jumps between frequencies. In addition, a strong relationship between neighboring frequencies is established, which includes the mean $\mu_S(\omega)$, the variance $\sigma_S^2(\omega)$ and the covariance $\varsigma_S(\omega, \omega + \Delta\omega)$ of the random variables of the respective spectral densities, resulting in a realistic representation of the data set. This procedure requires $N_\mathrm{Z} = N_\omega$ independent random variables, i.e. the randomly generated spectral density S_1 according to the respective PDF and a number of $N_\omega - 1$ random variables Φ_j.

4. Numerical examples

In the forthcoming section, the examination of numerical examples, including a linear oscillator and a nonlinear shear-frame structure, will be carried out to demonstrate the applicability of the dependency models described in Section 3. In addition, simulations are performed for the mean of the ensemble, an uncorrelated relaxed PSD function model and the individual estimated PSD functions of the ensemble, which are applied to the system under investigation in a MC simulation in order to obtain a benchmark result.

The ensemble considered in this work is an artificially generated ensemble. To emulate this ensemble, the Clough-Penzien PSD function model has been adopted to generate artificial stochastic processes by SRM (Eq. 8). The Clough-Penzien PSD function reads

$$S^{\mathrm{CP}}(\omega, S_0, \omega_\mathrm{f}, \zeta_\mathrm{f}, \omega_\mathrm{g}, \zeta_\mathrm{g}) = S_0 \cdot \frac{\omega^4}{(\omega_\mathrm{f}^2 - \omega^2)^2 + 4\zeta_\mathrm{f}^2\omega_\mathrm{f}^2\omega^2} \cdot \frac{\omega_\mathrm{g}^4 + 4\zeta_\mathrm{g}^2\omega_\mathrm{g}^2\omega^2}{(\omega_\mathrm{g}^2 - \omega^2)^2 + 4\zeta_\mathrm{g}^2\omega_\mathrm{g}^2\omega^2}, \tag{20}$$

where the parameters $S_0 = 0.01\ \mathrm{m}^2/s^3$, $\omega_\mathrm{f} = 0.8\pi$ rad/s, $\zeta_\mathrm{f} = 0.6$, $\omega_\mathrm{g} = 8\pi$ rad/s and $\zeta_\mathrm{g} = 0.6$, adopted from [43] and characterizing stiff soil conditions, has been utilized. The upper cut-off frequency is set to $\omega_\mathrm{u} = 150$ rad/s. Based on this PSD function description, $N_\mathrm{E} = 30$ randomly generated stochastic processes with a time duration of $T = 10$ s and a time discretization $\Delta t = 0.0209$ s were generated by SRM (Eq. 8) and transformed back into the frequency domain using Welch's method (Eq. 5). The resulting ensemble of PSD functions exhibits some fluctuation due to the utilization of random variables in SRM, emulating the randomness in real data. The ensemble is given in Fig. 5, while the corresponding generated relaxed PSD function is given in Fig. 6.

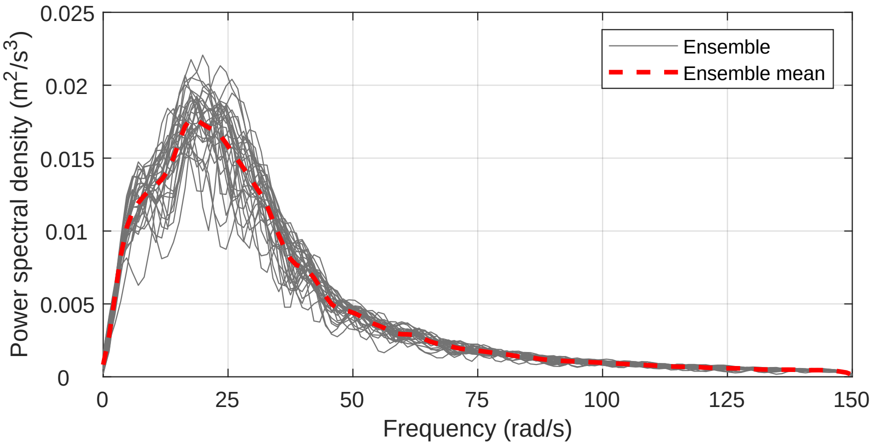

Figure 5: Ensemble of PSD functions utilized in this work.

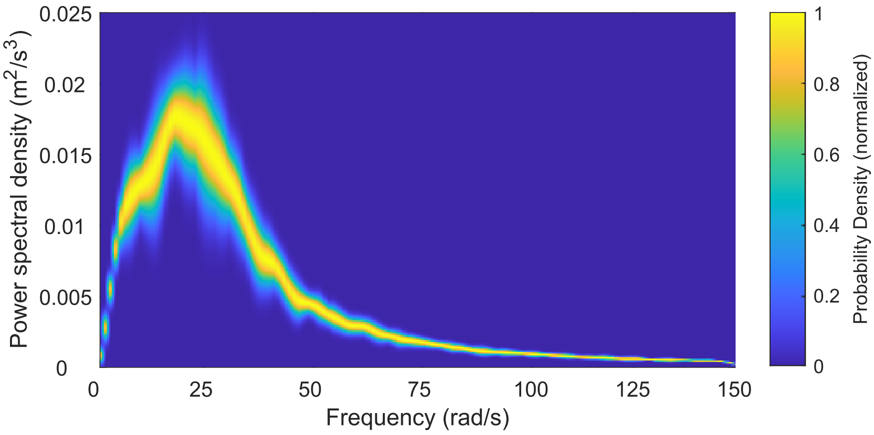

Figure 6: Relaxed PSD function generated from the ensemble of individual PSD functions.

4.1. Single degree of freedom (SDOF) system

A fully linear system without damping is considered for a proof-of-concept simulation. The equation of motion is

$$m\ddot{x}(t) + kx(t) = a_{\mathrm{g}}(t), \tag{21}$$

with mass $m = 5$ kg, stiffness $k = 1500$ N/m and $a_{\mathrm{g}}(t)$ as the stochastic ground motion acceleration of the system. The system is schematically depicted in Fig. 7. The failure probability is estimated through MC simulation and SuS, where exceeding the critical system displacement of $b_{\mathrm{crit}}^{\mathrm{SDOF}} = 0.1$ m is considered indicative of a system failure. For the MC simulation, 10^6 samples are used, while 10^4 samples are employed for SuS. The ground

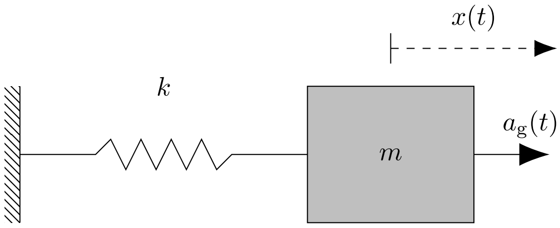

Figure 7: Schematic representation of the SDOF system.

Table 1: Failure probabilities of the SDOF system for the different dependency models.

Method	Benchmark	Mean	Uncorrelated	One RV	MVG	Proposed
MC	0.002746	0.000594	0.001616	0.003573	0.002593	0.002763
SuS	—	0.000539	0.001425	0.003584	0.002699	0.002662

motions $a_{\mathrm{g}}(t)$ are generated by SRM (Eq. 8) after sampling PSD functions utilizing the models described in Section 3.

The estimated failure probabilities are given in Table 1. It can be clearly seen that both the mean and the uncorrelated relaxed PSD function model underestimate the failure probability severely. In case of the mean even by an order of magnitude. The mean value model lacks the ability to produce PSD functions with high spectral densities, whether considered for the entire PSD function or for some frequencies. The uncorrelated model is able to sample such high spectral densities. However, since no correlations are taken into account, these are often equalised by sampling low spectral densities, so that in the end PSD functions are sampled that are similar in characteristics to the mean.

On the other hand, the models that take correlations or dependencies into account are significantly closer to the benchmark results. Merely the one RV model is too conservative and slightly overestimates the failure probability. This is due to the fact that using only one random variable may lead to often too PSD functions being sampled with high total energy, which are more likely to lead to system failure. Furthermore, since no correlations are taken into account in this model, but the dependencies are only modeled via one random variable, the model lacks a certain flexibility. Both, the MVG model and the proposed approach show a failure probability that corresponds very well with the benchmark result. As the proposed approach only considers the correlations between neighboring frequencies, its results are only a subset of the multivariate Gaussian variables. Nevertheless, the numerical results show that the proposed method achieves a considerable degree of accuracy. From this point of view, the proposed approach has the advantage of being sufficiently rational and efficient.

4.2. Nine storey shear-frame structure with nonlinear restoring force

For a more realistic case, a nonlinear nine storey shear-frame structure with $N_{\mathrm{f}} = 9$ degrees of freedom is considered in this section. The Bouc-Wen model [44, 45, 46] is adopted to represent the nonlinear behaviour of the structure. The governing equation of motion is

$$\mathbf{M}\ddot{\boldsymbol{x}}(t) + \mathbf{C}\dot{\boldsymbol{x}}(t) + \alpha\mathbf{K}\boldsymbol{x}(t) + (1-\alpha)\mathbf{H}\boldsymbol{z}(t) = -\mathbf{MI}a_{\mathrm{g}}(t), \tag{22}$$

where $\mathbf{M} \in \mathbb{R}^{N_{\mathrm{f}}\times N_{\mathrm{f}}}$ is the mass matrix, $\mathbf{C} \in \mathbb{R}^{N_{\mathrm{f}}\times N_{\mathrm{f}}}$ is the damping matrix, $\mathbf{K} \in \mathbb{R}^{N_{\mathrm{f}}\times N_{\mathrm{f}}}$ is the stiffness matrix, $\mathbf{H} \in \mathbb{R}^{N_{\mathrm{f}}\times N_{\mathrm{f}}}$ is the hysteretic matrix, $\mathbf{I} \in \mathbb{R}^{N_{\mathrm{f}}\times N_{\mathrm{f}}}$ is the identity matrix, and $a_{\mathrm{g}}(t)$ is a stochastic ground motion acceleration. The quantities $\ddot{\boldsymbol{x}}$, $\dot{\boldsymbol{x}}$, $\boldsymbol{x} \in \mathbb{R}^{1\times N_{\mathrm{f}}}$ describe the vectors of acceleration, velocity and displacement for each storey, respectively, $\boldsymbol{z} \in \mathbb{R}^{1\times N_{\mathrm{f}}}$ is a pseudo-displacement, see for instance [47], and α is the ratio between linear and nonlinear system behavior. The specific values for mass and stiffness for each storey are given in Table 2 and are adopted from [12] with a minor modification. Classical Rayleigh damping is assumed with $\mathbf{C} = a_1\mathbf{M} + a_2\mathbf{K}$, where a_1 and a_2 are computed from the first two eigenfrequencies $\omega_0^{(1)}$ and $\omega_0^{(2)}$ with damping ratio $\zeta = 5\%$, i.e. $a_1 = 2\zeta\omega_0^{(1)}\omega_0^{(2)}/(\omega_0^{(1)} + \omega_0^{(2)})$ and $a_2 = 2\zeta/(\omega_0^{(1)} + \omega_0^{(2)})$. The utilized Bouc-Wen model parameters are $\alpha = 0.01$, $A = 1$, $\beta = 1.4$, $\gamma = 0.2$, $n = 1$, $\delta_v = 0.002$, $\delta_\eta = 0.001$, $\zeta_s = 0.95$, $q = 0.25$, $p = 2$, $\Psi = 0.2$, $\delta_\psi = 0.005$ and $\lambda = 0.1$ and are adopted from [47], to which reference is also made for an explanation of the parameters. The stochastic ground motions $a_{\mathrm{g}}(t)$ are generated via SRM (Eq. 8) after sampling PSD functions via the described correlation models in Section 3. An inter-storey drift between the first and second storey of more than $b_{\mathrm{crit}}^{\mathrm{BW}} = 0.1$ m is considered as system failure. An example of a sampled PSD function with the proposed method, a generated stochastic process and the resulting nonlinear system behavior are

Table 2: Mass and lateral stiffness of the shear-frame structure model for the individual storeys.

Storey no.	1	2	3	4	5	6	7	8	9
Mass ($\times 10^6$ kg)	3.5	3.3	3.0	3.0	3.0	3.0	3.0	2.7	2.7
Stiffness ($\times 10^8$ N/m)	1.47	1.63	1.62	1.60	1.60	1.92	1.85	0.96	0.89

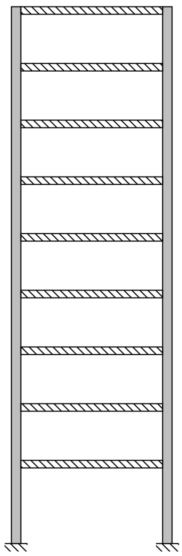

Figure 8: Schematic representation of the nine storey shear-frame structure.

depicted in Fig. 9. Again, the simulations are carried out by MC simulation with 10^6 and SuS with 10^4 samples.

The estimated failure probabilities are provided in Table 3. This setup shows a similar trend as the SDOF model, which also confirms the previous results. While the mean model underestimate the failure probability by an order of magnitude, the uncorrelated model performs better as in the SDOF model simulation but is still not very accurate. The one RV model is again overestimating the failure probability, which leads to the conclusion that this model is generally too conservative. The results of the MVG model and the proposed correlation model show a clear consistency with the benchmark result and have a remarkable accuracy, which confirms that the consideration of correlations and the modeling of dependencies is crucial in failure probability estimation.

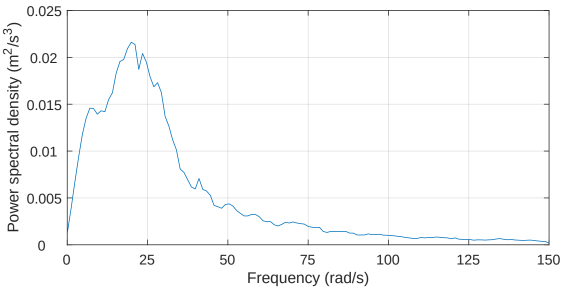

(a)

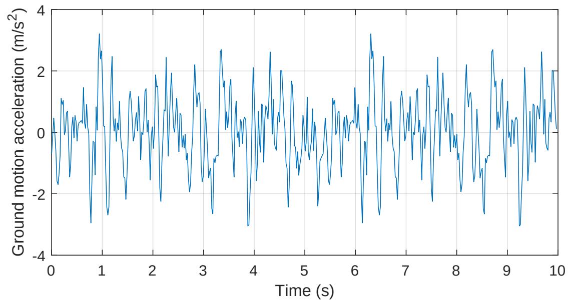

(b)

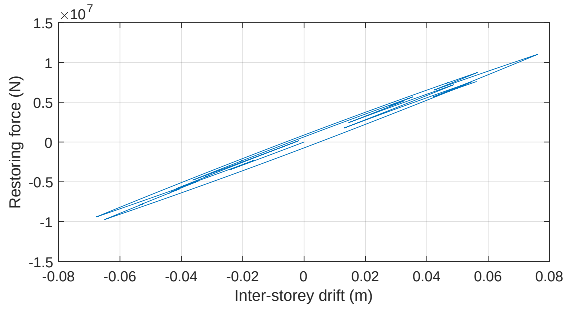

(c)

Figure 9: A PSD function sampled by the proposed method (a); a sample of a stationary ground motion acceleration generated with SRM (Eq. 8) (b); and the resulting inter-storey drift vs. restoring force of the shear-frame structure (c).

4.3. Limitations

A limitation of the dependency models is that they are conditional on a certain level of correlation within the data set for accurate failure probability estimation. When there is no correlation or the correlation is too low, the simulation results align with the mean value or an uncorrelated model, leading to results of poor quality. To illustrate this issue, the SDOF model with MC simulation is run again with a data set estimated using the periodogram (Eq. 2), which is generally considered a poor estimator. The results are shown in Table 4. In instances where correlations are low, PSD functions with high variation are consistently sampled, regardless of the approach employed, as depicted in Fig. 10. Consequently, all methods yield similar results that align with the benchmark. However, as the benchmark itself has a low correlation, the quality of these results is not reliable.

Table 3: Failure probabilities of the shear-frame structure model for the different dependency models.

Method	Benchmark	Mean	Uncorrelated	One RV	MVG	Proposed
MC	0.014642	0.005426	0.012289	0.01701	0.014473	0.015085
SuS	—	0.00591	0.01242	0.01706	0.01481	0.01472

Table 4: Failure probabilities of the SDOF system for the different dependency models by utilising a data set with low correlation.

Method	Benchmark	Mean	Uncorrelated	One RV	MVG	Proposed
MC	0.043357	0.043022	0.043595	0.045229	0.043279	0.042622

5. Conclusions

In this work, the dependency modeling and sampling between frequencies in the relaxed PSD function was investigated and a novel approach tailored for this purpose was proposed. The analysis indicates that estimated failure probabilities, when considering correlations and dependencies, are much more accurate and can differ by an order of magnitude compared to uncorrelated models. This underscores the importance of incorporating correlations and model dependencies for a more accurate assessment of failure probabilities. Simulations of individual PSD functions support the realism of models that account for dependencies, showing comparable failure probabilities to correlation models. In contrast, uncorrelated models, providing only averaged results, tend to be overly optimistic and systematically underestimate failure probabilities. The limitations of uncorrelated models become evident in their failure to systematically address the complexity and uncertainty inherent in the data, prompting questions about their reliability in predicting failure probabilities. The investigation highlights a potential over-conservatism in the one RV model. Conversely, both the MVG model and the proposed approach are effective due to the inclusion of correlations, whereby these approaches emerging as favored due to their highest consistency with the benchmark simulations. Since the MVG model and the proposed approach are able to estimate a more nuanced failure probability, this has a direct impact on real-world phenomena

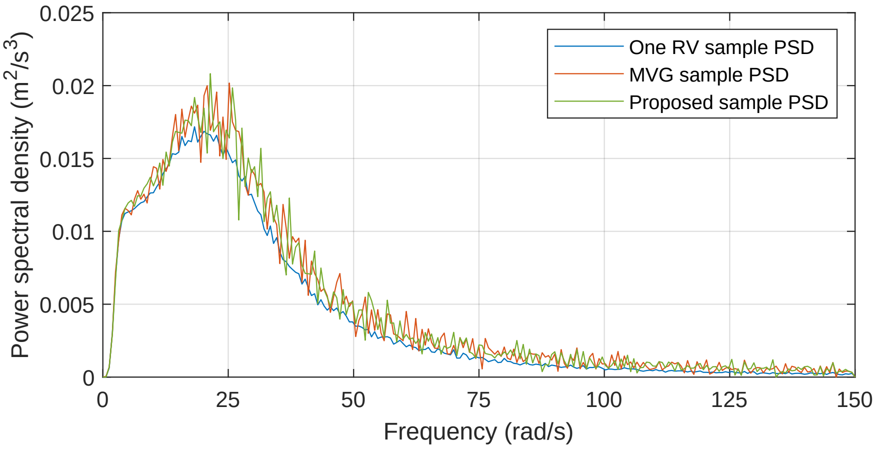

Figure 10: Sampled PSD functions from the relaxed PSD of a data set with low correlation.

and decision making in dynamic systems. The more accurate failure probability is higher than the failure probability of the mean or uncorrelated model, which directly impacts decisions on the reliability of the system and building, for instance decisions on the material used to make it resistant to certain loads. With the improved estimation of the failure probability, buildings and structures can be better designed in accordance with the simulation results based on the dependency models. In conclusion, this research underscores the necessity of considering correlations when modeling relaxed PSD functions, as uncorrelated models demonstrate inadequacies in capturing the nuanced aspects of failure probabilities.

Acknowledgement

This work was supported by the National Natural Science Foundation of China (Grant No. 12302037); the China Postdoctoral Science Foundation (Grant No. 2023M732669); the Shanghai Post-Doctoral Excellence Program (Grant No. 2022558); and the European Union's Horizon 2020 research and innovation programme under Marie Sklodowska-Curie project GREYDIENT – Grant Agreement n°955393.

References

[1] Y.-K. Lin, G.-Q. Cai, Probabilistic Structural Dynamics: Advanced Theory and Applications, McGraw-Hill New York, 1995.

[2] A. K. Chopra, Dynamics of Structures: Theory and Applications to Earthquake Engineering, Prentice-Hall, 1995.

[3] J. Li, J. Chen, Stochastic Dynamics of Structures, John Wiley & Sons, 2009.

[4] M. Grigoriu, Stochastic Calculus, Birkhäuser Boston, Boston, MA, 2002. URL: http://link.springer.com/10.1007/978-0-8176-8228-6. doi:10.1007/978-0-8176-8228-6.

[5] A. Powell, S. Crandall, Random Vibration, The Technology Press of the Massachusetts Institute of Technology, Cambridge, 1958.

[6] T. T. Soong, M. Grigoriu, Random Vibration of Mechanical and Structural Systems, Prentice-Hall, 1993.

[7] J. B. Roberts, P. D. Spanos, Random vibration and statistical linearization, Courier Corporation, 2003.

[8] L. D. Lutes, S. Sarkani, Random Vibrations: Analysis of Structural and Mechanical Systems, Butterworth-Heinemann, 2004.

[9] D. E. Newland, An Introduction to Random Vibrations, Spectral & Wavelet Analysis, Courier Corporation, 2012.

[10] R. A. Muller, G. J. MacDonald, Ice ages and astronomical causes: data, spectral analysis and mechanisms, Springer Science & Business Media, 2002.

[11] M. Shinozuka, G. Deodatis, Simulation of stochastic processes by spectral representation, Applied Mechanics Reviews 44 (1991) 191–204. doi:10.1115/1.3119501.

[12] J. Chen, W. Sun, J. Li, J. Xu, Stochastic Harmonic Function Representation of Stochastic Processes, Journal of Applied Mechanics 80 (2013) 011001. URL: https://asmedigitalcollection.asme.org/appliedmechanics/article/doi/10.1115/1.4006936/367667/Stochastic-Harmonic-Function-Representation-of. doi:10.1115/1.4006936, number: 1.

[13] J. Chen, L. Comerford, Y. Peng, M. Beer, J. Li, Reduction of random variables in the stochastic harmonic function representation via spectrum-relative dependent random frequencies, Mechanical Systems and Signal Processing 141 (2020) 106718. URL: http://www.sciencedirect.com/science/article/pii/S0888327020301047. doi:https://doi.org/10.1016/j.ymssp.2020.106718.

[14] A. D. Kiureghian, O. Ditlevsen, Aleatory or epistemic? does it matter?, Structural Safety 31 (2009) 105–112. URL: https://www.sciencedirect.com/science/article/pii/S0167473008000556. doi:https://doi.org/10.1016/j.strusafe.2008.06.020, risk Acceptance and Risk Communication.

[15] E. Nikolaidis, D. M. Ghiocel, S. Singhal, Engineering Design Reliability Handbook, 1 ed., CRC press, 2004. doi:https://doi.org/10.1201/9780203483930.

[16] J. Chen, Z. Wan, A compatible probabilistic framework for quantification of simultaneous aleatory and epistemic uncertainty of basic parameters of structures by synthesizing the change of measure and

change of random variables, Structural Safety 78 (2019) 76 – 87. URL: http://www.sciencedirect.com/science/article/pii/S0167473018303059. doi:https://doi.org/10.1016/j.strusafe.2019.01.001.

[17] S. Bi, M. Broggi, M. Beer, The role of the Bhattacharyya distance in stochastic model updating, Mechanical Systems and Signal Processing 117 (2019) 437–452. URL: https://www.sciencedirect.com/science/article/pii/S0888327018304837. doi:https://doi.org/10.1016/j.ymssp.2018.08.017.

[18] G. I. Schuëller, On the treatment of uncertainties in structural mechanics and analysis, Computers & Structures 85 (2007) 235–243.

[19] M. Grigoriu, Stochastic Systems: Uncertainty Quantification and Propagation, Springer Series in Reliability Engineering, Springer London, London, 2012. URL: https://link.springer.com/10.1007/978-1-4471-2327-9. doi:10.1007/978-1-4471-2327-9.

[20] R. Ghanem, D. Higdon, H. Owhadi (Eds.), Handbook of Uncertainty Quantification, Springer International Publishing, Cham, 2017. URL: http://link.springer.com/10.1007/978-3-319-12385-1. doi:10.1007/978-3-319-12385-1.

[21] C. Soize, Uncertainty Quantification: An Accelerated Course with Advanced Applications in Computational Engineering, volume 47 of *Interdisciplinary Applied Mathematics*, Springer International Publishing, Cham, 2017. URL: http://link.springer.com/10.1007/978-3-319-54339-0. doi:10.1007/978-3-319-54339-0.

[22] M. G. Faes, D. Moens, Recent trends in the modeling and quantification of non-probabilistic uncertainty, Archives of Computational Methods in Engineering 27 (2020) 633–671. URL: https://link.springer.com/article/10.1007/s11831-019-09327-x. doi:https://doi.org/10.1007/s11831-019-09327-x.

[23] M. Beer, S. Ferson, V. Kreinovich, Imprecise probabilities in engineering analyses, Mechanical Systems and Signal Processing 37 (2013) 4–29. URL: https://linkinghub.elsevier.com/retrieve/pii/S0888327013000812. doi:10.1016/j.ymssp.2013.01.024, number: 1-2.

[24] E. Zio, The Monte Carlo Simulation Method for System Reliability and Risk Analysis, Springer Series in Reliability Engineering, Springer London, London, 2013. URL: https://link.springer.com/10.1007/978-1-4471-4588-2. doi:10.1007/978-1-4471-4588-2.

[25] G. I. Schuëller, Efficient Monte Carlo simulation procedures in structural uncertainty and reliability analysis - recent advances, Structural Engineering and Mechanics 32 (2009) 1–20.

[26] S.-K. Au, J. L. Beck, Estimation of small failure probabilities in high dimensions by subset simulation, Probabilistic Engineering Mechanics 16 (2001) 263–277. URL: https://www.sciencedirect.com/science/article/pii/S0266892001000194. doi:https://doi.org/10.

1016/S0266-8920(01)00019-4.

[27] S. Au, Reliability-based design sensitivity by efficient simulation, Computers & Structures 83 (2005) 1048–1061. URL: https://www.sciencedirect.com/science/article/pii/S0045794905000398. doi:https://doi.org/10.1016/j.compstruc.2004.11.015, uncertainties in Structural Mechanics and Analysis–Computational Methods.

[28] M. de Angelis, E. Patelli, M. Beer, Advanced line sampling for efficient robust reliability analysis, Structural Safety 52 (2015) 170–182. URL: https://www.sciencedirect.com/science/article/pii/S0167473014000927. doi:https://doi.org/10.1016/j.strusafe.2014.10.002, engineering Analyses with Vague and Imprecise Information.

[29] C. Dang, M. A. Valdebenito, M. G. Faes, P. Wei, M. Beer, Structural reliability analysis: A Bayesian perspective, Structural Safety 99 (2022) 102259. URL: https://linkinghub.elsevier.com/retrieve/pii/S0167473022000674. doi:10.1016/j.strusafe.2022.102259.

[30] C. Dang, M. A. Valdebenito, M. G. Faes, J. Song, P. Wei, M. Beer, Structural reliability analysis by line sampling: A Bayesian active learning treatment, Structural Safety 104 (2023) 102351. URL: https://linkinghub.elsevier.com/retrieve/pii/S0167473023000383. doi:10.1016/j.strusafe.2023.102351.

[31] L. Comerford, I. A. Kougioumtzoglou, M. Beer, An artificial neural network approach for stochastic process power spectrum estimation subject to missing data, Structural Safety 52 (2015) 150–160. URL: https://linkinghub.elsevier.com/retrieve/pii/S0167473014000915. doi:10.1016/j.strusafe.2014.10.001.

[32] L. Comerford, I. A. Kougioumtzoglou, M. Beer, On quantifying the uncertainty of stochastic process power spectrum estimates subject to missing data, International Journal of Sustainable Materials and Structural Systems 2 (2015) 185. URL: http://www.inderscience.com/link.php?id=78358. doi:10.1504/IJSMSS.2015.078358, number: 1/2.

[33] Y. Zhang, L. Comerford, I. A. Kougioumtzoglou, E. Patelli, M. Beer, Uncertainty Quantification of Power Spectrum and Spectral Moments Estimates Subject to Missing Data, ASCE-ASME Journal of Risk and Uncertainty in Engineering Systems, Part A: Civil Engineering 3 (2017) 04017020. URL: https://ascelibrary.org/doi/10.1061/AJRUA6.0000925. doi:10.1061/AJRUA6.0000925, number: 4.

[34] L. Comerford, I. A. Kougioumtzoglou, M. Beer, Compressive sensing based stochastic process power spectrum estimation subject to missing data, Probabilistic Engineering Mechanics 44 (2016) 66–76. URL: https://linkinghub.elsevier.com/retrieve/pii/S0266892015300436. doi:10.1016/j.probengmech.2015.09.015.

[35] L. Comerford, H. Jensen, F. Mayorga, M. Beer, I. Kougioumtzoglou, Compressive sensing with an

adaptive wavelet basis for structural system response and reliability analysis under missing data, Computers & Structures 182 (2017) 26–40. URL: https://linkinghub.elsevier.com/retrieve/pii/S0045794916304618. doi:10.1016/j.compstruc.2016.11.012.

[36] M. G. Faes, M. A. Valdebenito, D. Moens, M. Beer, Bounding the first excursion probability of linear structures subjected to imprecise stochastic loading, Computers & Structures 239 (2020) 106320. URL: https://www.sciencedirect.com/science/article/pii/S0045794920301231. doi:https://doi.org/10.1016/j.compstruc.2020.106320.

[37] M. Behrendt, M. G. Faes, M. A. Valdebenito, M. Beer, Estimation of an imprecise power spectral density function with optimised bounds from scarce data for epistemic uncertainty quantification, Mechanical Systems and Signal Processing 189 (2023) 110072. URL: https://www.sciencedirect.com/science/article/pii/S0888327022011402. doi:https://doi.org/10.1016/j.ymssp.2022.110072.

[38] G. Muscolino, F. Genovese, A. Sofi, Reliability Bounds for Structural Systems Subjected to a Set of Recorded Accelerograms Leading to Imprecise Seismic Power Spectrum, ASCE-ASME Journal of Risk and Uncertainty in Engineering Systems, Part A: Civil Engineering 8 (2022) 04022009. doi:10.1061/AJRUA6.0001215.

[39] M. Behrendt, M. Bittner, L. Comerford, M. Beer, J. Chen, Relaxed power spectrum estimation from multiple data records utilising subjective probabilities, Mechanical Systems and Signal Processing 165 (2022) 108346. URL: https://linkinghub.elsevier.com/retrieve/pii/S0888327021007020. doi:10.1016/j.ymssp.2021.108346.

[40] M. S. Bartlett, Smoothing periodograms from time-series with continuous spectra, Nature 161 (1948) 686–687.

[41] M. S. Bartlett, Periodogram analysis and continuous spectra, Biometrika 37 (1950) 1–16. URL: https://doi.org/10.1093/biomet/37.1-2.1. doi:10.1093/biomet/37.1-2.1. arXiv:https://academic.oup.com/biomet/article-pdf/37/1-2/1/486591/37-1-2-1.pdf.

[42] P. Welch, The use of fast Fourier transform for the estimation of power spectra: A method based on time averaging over short, modified periodograms, IEEE Transactions on Audio and Electroacoustics 15 (1967) 70–73. doi:10.1109/TAU.1967.1161901.

[43] G. Deodatis, Non-stationary stochastic vector processes: seismic ground motion applications, Probabilistic Engineering Mechanics 11 (1996) 149–167. URL: https://www.sciencedirect.com/science/article/pii/0266892096000070. doi:https://doi.org/10.1016/0266-8920(96)00007-0.

[44] R. Bouc, Forced vibrations of mechanical systems with hysteresis, in: Proc. of the Fourth Conference on Nonlinear Oscillations, Prague, 1967, 1967.

[45] Y.-K. Wen, Method for random vibration of hysteretic systems, Journal of the engineering mechanics division 102 (1976) 249–263.

[46] T. T. Baber, Y.-K. Wen, Random vibration hysteretic, degrading systems, Journal of the Engineering Mechanics Division 107 (1981) 1069–1087.

[47] F. Ma, H. Zhang, A. Bockstedte, G. C. Foliente, P. Paevere, Parameter analysis of the differential model of hysteresis, Journal of Applied Mechanics 71 (2004) 342–349.